Monomolecular films of arborescent polystyrene–*graft*–poly(2-vinylpyridine) copolymers: Precursors to nanostructured carbon materials

Mongyoung Huh,[1] Mario Gauthier,[2] Seok Il Yun[3*]

[1]Korea Institute of Carbon Convergence Technology, Jeonju 561-844, Republic of Korea

[2]Department of Chemistry, Waterloo Institute for Nanotechnology and Institute for Polymer Research, University of Waterloo, Waterloo, Ontario N2L 3G1, Canada

[3]Department of Chemical Engineering and Materials Science, Sangmyung University, Seoul 110-743, Republic of Korea*

ABSTRACT: An arborescent polystyrene (PS)–*graft*–poly(2-vinylpyridine) (P2VP) copolymer of overall generation number G2, consisting of side chains with M_n ~5000, served as template for the preparation of nanostructured carbon films. Spin casting of arborescent PS–*graft*–P2VP copolymers yielded monomolecular films of uniform thickness. The uniformity of the copolymer films was influenced by the casting solvent selected. Methanol solutions of the copolymers led to non-uniform layers consisting of large aggregates and voids. Homogeneous monolayer films were attained from copolymer solutions in tetrahydrofuran, which is a good solvent for both the PS and P2VP components. The copolymer molecules in the film were strongly flattened by adsorption forces, but recovered a spherical geometry after annealing in water. The water-annealed films could be directly converted into their analogous carbon films having nanodots on the surface by UV irradiation with concurrent pyrolysis. The

* Corresponding author. Tel: 02 781-7530 E-mail: yunsans@smu.ac.kr (Seok Il Yun)

pyrolyzed nanomaterials exhibited the characteristics of partially graphitic carbon with nitrogen.

Introduction

Arborescent graft polymers (AGP) are highly branched macromolecules synthesized via successive cycles of polymer chain functionalization and grafting [1]. An important feature of AGP that distinguishes them from other dendritic polymer families, such as hyperbranched and dendrimer molecules, is the incorporation of linear polymer chains rather than monomers as building blocks. This synthetic strategy yields branched polymers with very high molecular weights in a few grafting cycles (generations), while maintaining a narrow molecular weight distribution. Arborescent graft polystyrene (AGPS) molecules obtained by that approach were shown to have an increasingly hard-sphere morphology in solution as the generation number (G) increased or the side chain length decreased [2]. Spin casting of AGPS solutions led to monolayers of distinct hexagonally packed globular structures on planar substrates [3]. The AGP used in the current investigation was a copolymer consisting in an arborescent PS core and a large number of covalently bonded P2VP chains forming a shell (arborescent PS–*graft*–P2VP), depicted as unimolecular micelles in Figure 1a [4]. The solution properties of arborescent PS–*graft*–P2VP copolymers have been investigated extensively [5], but structural investigations of these unimolecular micelles in films have not yet been performed. Ordered micellar films have received much attention in nanotechnology, however the polymeric micelles used are mostly derived from amphiphilic linear block copolymers (BCP), in a solvent selective for one of the components forming the shell. The covalently bonded structure of unimolecular micelles is advantageous when colloidal stability is required under conditions unsuitable for BCP micelles. Other notable features of unimolecular micelles

include the absence of a critical micelle concentration and the lack of requirement for phase separation between the components. Phase-separated BCP materials were applied as precursors to be pyrolyzed into carbon nanomaterials [6–19]. In particular, the pyrolysis of a BCP having one block composed of nitrogen-containing species, such as polyvinylpyridine or poly(acrylonitrile) (PAN), can directly produce carbon nanostructures enriched with nitrogen [9–19], that displayed remarkable electro-catalytic activity in the oxygen reduction reaction (ORR) [20–22]. In addition to the ORR, N-doped carbon has shown significant electrochemical activity in other applications such as semiconductors, lithium ion batteries and ultracapacitors [21,22]. In this work, an ordered micellar monolayer of arborescent PS–*graft*–P2VP copolymer was obtained by spin casting. It was hypothesized that the AGP could serve as precursor to be pyrolyzed into carbon nanomaterials, due to its high branching density and structural stability. The PS core and P2VP shell were crosslinked by UV irradiation [12,14]. Pyrolysis of the photo-crosslinked arborescent copolymer films yielded nitrogen-enriched nanostructured carbon films. Our work is the first report on the successful preparation of nanostructured carbonaceous films from unimolecular micelles.

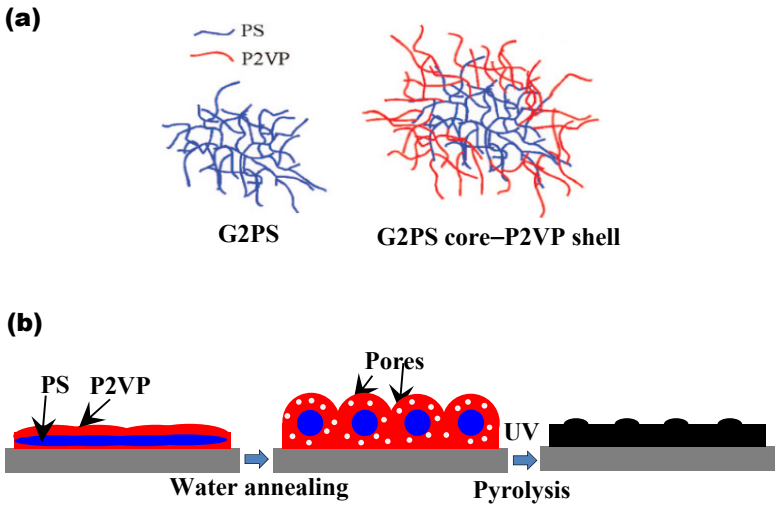

Figure 1. (a) Schematic representation of arborescent PS–*graft*–P2VP copolymers; (b) preparation of nanostructured carbonaceous films bearing carbon nanodot arrays by direct crosslinking and carbonization of a monolayer of PS–*graft*–P2VP copolymers.

Experimental section

The synthesis of the arborescent PS–*graft*–P2VP copolymers of the type used in the current investigation was described previously [4]. Arborescent PS–*graft*–P2VP copolymers of low generations (G0 or G1) or with long side chains (M_n ~30,000) only yielded heterogeneous films. In this study, an arborescent PS–*graft*–P2VP copolymer of overall generation G2, consisting of side chains with M_n ~5000, was used as template for the nanostructured carbon films. This sample was selected because it maintained a more stable spherical morphology, and formed more homogeneous layers on the solid substrate than the G0 and G1 copolymers.

A twice-grafted arborescent polystyrene (Generation 1 polystyrene, G1PS), containing 205 side chains with $M_n = 4900$ and having a total $M_n = 1.1 \times 10^6$, served as grafting substrate

to prepare the copolymer. A total of 1180 side chains of P2VP (M_n = 6200) were grafted onto the G1PS substrate, to give and arborescent PS–*graft*–P2VP copolymer of overall generation G2, with a total $M_n = 8.4 \times 10^6$ and $M_w/M_n = 1.09$. The number-average molecular weight (M_n) was determined by gel permeation chromatography analysis of the sample with a multi-angle laser light scattering detector. The number of side chains was calculated according to the equation $f_n(\text{total}) = f_n(G-1) + [M_n(G) - M_n(G-1)] / [M_n(\text{branch})]$, where $M_n(G)$, $M_n(G-1)$, and M_n(branch) represent the number-average relative molecular weights of polymers of generation G, of the previous generation, and of the side chains, respectively. The micellar films were prepared on silicon wafers by spin casting of an arborescent PS–*graft*–P2VP copolymer solution in methanol or in tetrahydrofuran (THF). The Si wafers were cleaned by piranha solution etching prior to casting. The spin cast films were dried in a fume hood. The arborescent PS–*graft*–P2VP thin films were exposed to 254 nm UV light for 2 h to induce crosslinking of the PS core and the P2VP shell. The crosslinked copolymer films were then subjected to pyrolysis under Ar gas at 600 °C for 20 min. The topology of the precursor and carbonaceous films was studied by tapping-mode atomic force microscopy (AFM, Dimension 3100S, Veeco). Scanning electron microscopy (SEM, Hitachi S-5500 FE-SEM) was used to characterize the arborescent copolymer thin films before and after carbonization. The formation of carbonaceous material was confirmed by Raman scattering spectroscopy (Integra Spectra II, NT-MDT SI), and the analysis of the chemical components in the carbonaceous films was performed by X-ray photoelectron spectroscopy (XPS, Escalab 220xi, Thermo Fisher Scientific).

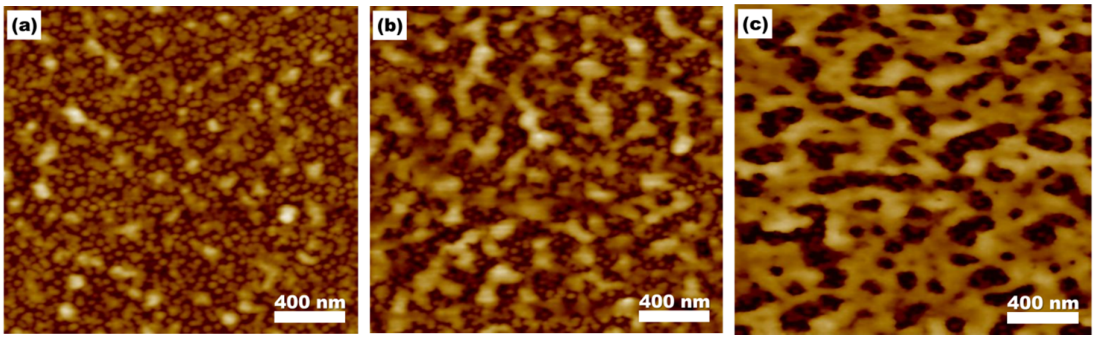

Figure 2. AFM images for thin films cast from arborescent PS–*graft*–P2VP copolymer solutions in methanol as a function of copolymer concentration: (a) 0.1, (b) 0.25, and (c) 1 wt%.

Results and Discussion

Two different solvents, methanol and THF, were investigated to cast the polymer films. The thin films were prepared from copolymer solutions at different concentrations (ϕ). In general, the solvent selected plays a very important role in inducing the phase separation of BCPs to form micelles [23]. Furthermore, BCPs can reorganize into different nanostructures by solvent vapor annealing of the films after the micelles are transferred onto a substrate [12,23]. Such strong solvent-dependent structural variations of the type observed for BCP seems unlikely for arborescent copolymers however, because of the fixed core-shell morphology of these unimolecular micelle resulting from covalent binding of the components. Nevertheless, the regularity of the arborescent copolymer arrays formed in the films *was* largely influenced by the choice of solvent. AFM images obtained for the arborescent PS–*graft*–P2VP copolymer films cast from methanol solutions are provided in Figure 2 as a function of ϕ. As can be seen, the arborescent copolymer molecules formed aggregates in the film, and the aggregates and voids became substantially larger as the polymer concentration was increased. While methanol

is a selective solvent for P2VP, the arborescent PS–*graft*–P2VP copolymers are known to disperse uniformly in methanol within the ϕ range investigated (0.1 < ϕ < 1 %) [5]. It is likely that the PS cores strongly attract each other during evaporation of the methanol, leading to the large aggregates and voids observed in the film. Exposing the arborescent PS–*graft*–P2VP copolymer films to solvent vapor annealing with THF, a good solvent for both PS and P2VP, did not significantly alter the morphology of the films cast from methanol solutions.

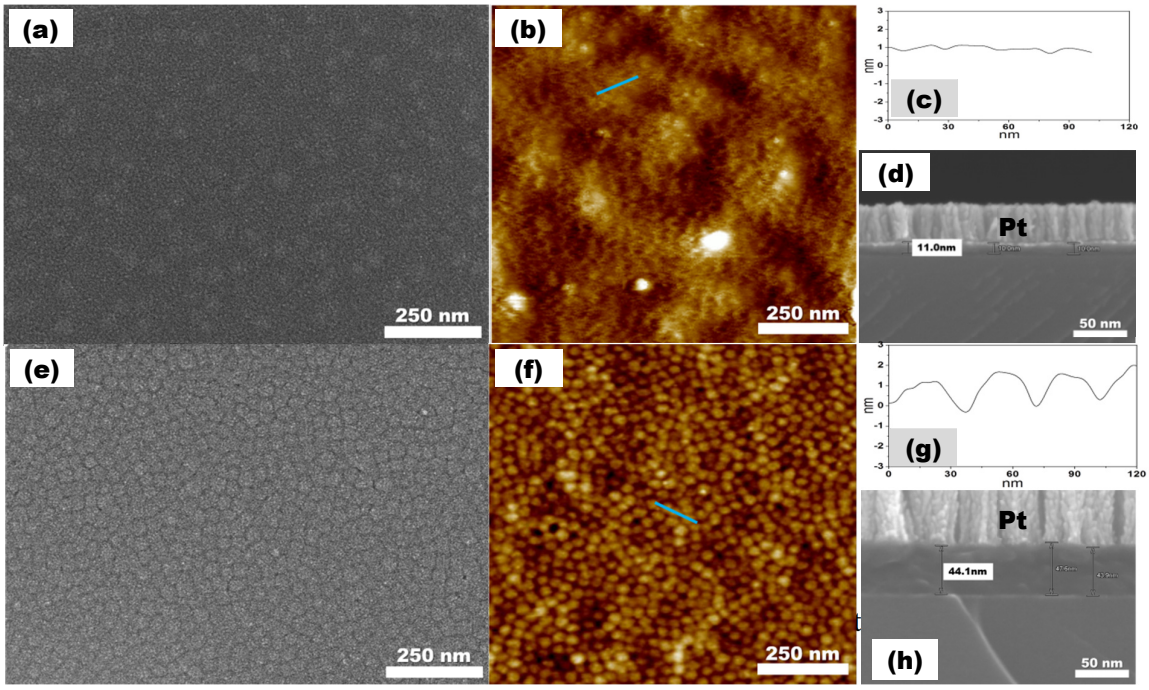

Figure 3. Micellar films cast from arborescent PS–*graft*–P2VP copolymer solutions in THF at ϕ = 0.1 wt%: (a) SEM image, (b) AFM topography image, (c) apparent topographic AFM profile taken along the line in (b), and (d) cross-sectional SEM image. Water-treated film cast from PS–*graft*–P2VP copolymers in THF at ϕ = 0.1 wt%: (e) SEM image, (f) AFM topography image, (g) apparent topographic AFM profile taken along the line in (f), and (h) cross-sectional SEM image. Pt was deposited on the copolymer film surface to emphasize the cross-section. The scan size is 1 μm × 1 μm for both AFM images, and the height scale is 20 nm.

As shown in Figure 3, the arborescent PS–*graft*–P2VP copolymer deposited from the THF solution ($\phi = 0.1$ wt%) formed a uniform layer on the planar surface, which contrasts with the result obtained using methanol. The corresponding SEM image, AFM topography image and topographic profile of the as-cast films are provided in Figure 3a–c, respectively. It can be seen that the P2VP shell of adjacent arborescent copolymer molecules interpenetrate to give diffuse interfaces (Figures 3a and 3b), making it difficult to determine the dimensions of individual copolymer molecules from the SEM and AFM images. The apparent peak-to-valley height, determined from the topographic AFM profile shown in Figure 3c, measured along the line depicted in Figure 3b, was approximately 0.26 ± 0.05 nm. From the cross-sectional SEM image (Figure 3d), the overall film thickness was measured to be approximately 11 ± 0.8 nm. A hypothetical hardcore diameter of 30 nm was calculated for the arborescent PS–*graft*–P2VP copolymer, based on a number-average molar mass of 8.4×10^6 and a collapsed sphere topology. These results clearly indicate that copolymers are flattened on the substrate, due to strong interactions between the P2VP shell chains and the polar piranha-etched Si surface. The as-cast film from the THF solution ($\phi = 0.1$ wt%) was soaked in water for 30 min and dried. With this treatment, the individual copolymer molecules did not coalesce but remained relatively distinct (Figures 3b1 and 3b2). The lateral size of the copolymer molecules was measured to be about 35 nm from SEM (Figure e) and AFM (Figures 3f). Notably, the film thickness and apparent peak-to-valley height increased to 44 ± 2 nm and $1.6_4 \pm 0.3_6$ nm in the SEM (Figure 3h) and AFM (Figure 3g) analysis, respectively, after water treatment of the as-cast film. These results clearly show that the water annealing procedure modified the molecular dimensions of the copolymer molecules deposited on the substrate. Specifically the film thickness increased, and hence the height of the spheres. The highly flattened arborescent copolymer molecules thus recovered a spherical geometry upon annealing. While P2VP is

essentially hydrophobic in neutral water, significant rearrangements clearly still took place within the film, so water must have plasticized P2VP sufficiently to allow the molecules to relax and regain an almost spherical shape, in analogy to arborescent PS films with similar characteristics that were annealed thermally [3]. For the arborescent PS homopolymer systems, thermal annealing above the glass transition temperature (T_g) was shown to facilitate the recovery of a spherical geometry, but also led to the formation of defects (holes) in the films, which necessarily implied migration of the molecules on the substrate [3]. However, such holes or defects were not detected for water-annealed arborescent P2VP copolymer films. This can be explained by the different interactions with the substrate present in the two systems. The relatively nonpolar arborescent PS films were cast onto polar mica substrates, leading to relatively weak interactions between the two components. For the P2VP copolymers cast onto the piranha solution-etched silicon surface, the interactions between the polar P2VP component and Si-OH or Si=O groups on the substrate should be much stronger, which effectively prevented the migration of the molecules as in the case of the PS system. Since the film thickness increased from 11 nm to 44 nm upon annealing in water, it is postulated that a large number of small pores formed within the film during that process, that did not collapse during water evaporation, so the P2VP chains did not densely pack but became very porous as depicted in Figure 1b. Solvent annealing, inducing morphological changes, has not been reported previously for highly branched unimolecular micelles such as the arborescent copolymers.

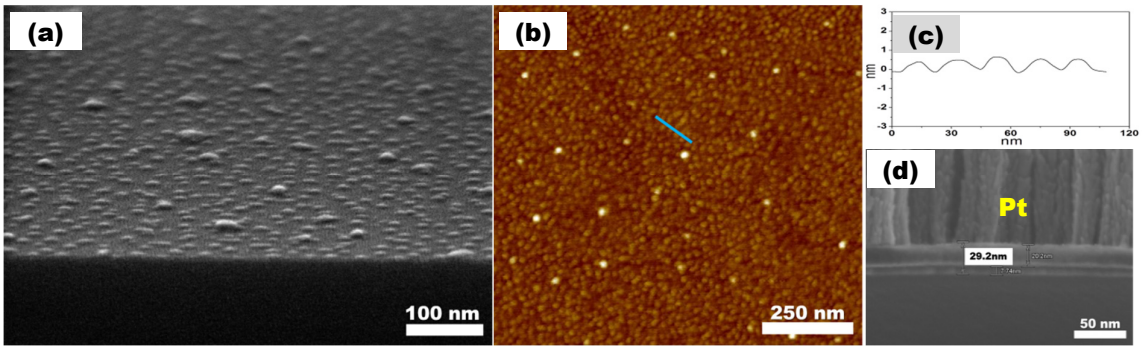

Figure 4. Carbonaceous film obtained by water annealing, crosslinking and pyrolysis at 600 °C for 20 min of film cast from PS–*graft*–P2VP copolymers in THF at ϕ = 0.1 wt%: (a) tilted SEM image, (b) AFM topography image, (c) apparent topographic AFM profile taken along the line in (b), and (d) cross-sectional SEM image with Pt deposited on the carbonized film surface to emphasize the cross-section.

As noted earlier, crosslinking the PS core and P2VP shell was induced by UV light before pyrolysis. This caused the photo-crosslinked core and shell to transform into carbon dots. A tilted SEM image for the carbonized film obtained is provided in Figure 4a. The pyrolysis without crosslinking by UV irradiation led to almost no features on the film (Not shown). Significant shrinkage occurred, as reflected by the smaller lateral size of the carbon dots (d = 16 ± 1 nm) as compared with the precursor (Figure 4a). Larger carbon dots with d = 29 ± 3 nm were also observed, indicating that some arborescent copolymer molecules coalesced during pyrolysis, resulting in decreased ordering of the carbon dots as compared with the precursor array. The carbonized film thickness measured from the cross-sectional SEM image (Figure 4d) was 29.2 nm, which indicates a volume shrinkage of approximately 34% in the direction perpendicular to the substrate surface. Additionally, relatively to the apparent peak-to-valley height of the as-cast film treated with water ($1.6_4 \pm 0.3_6$ nm, Figure 3g), the

height of the carbon nanoparticles in the film along the line depicted in the AFM image (Figure 4b) decreased to $0.6_1 \pm 0.2_0$ nm (Figure 4c). These findings suggest the formation of carbon nanodots on an underlying continuous carbon film, as previously reported for pyrolyzed BCP micellar film of PS–*block*–P2VP [7]. Therefore, the "dots-on-film" topography of the native arborescent PS–*graft*–P2VP template was preserved as depicted in Figure 1b. Notably, it was difficult to discern carbon nanodots when the as-cast films were not subjected to water treatment prior to UV exposure, because pyrolysis of the relatively flat as-casted copolymer films yielded a very low height.

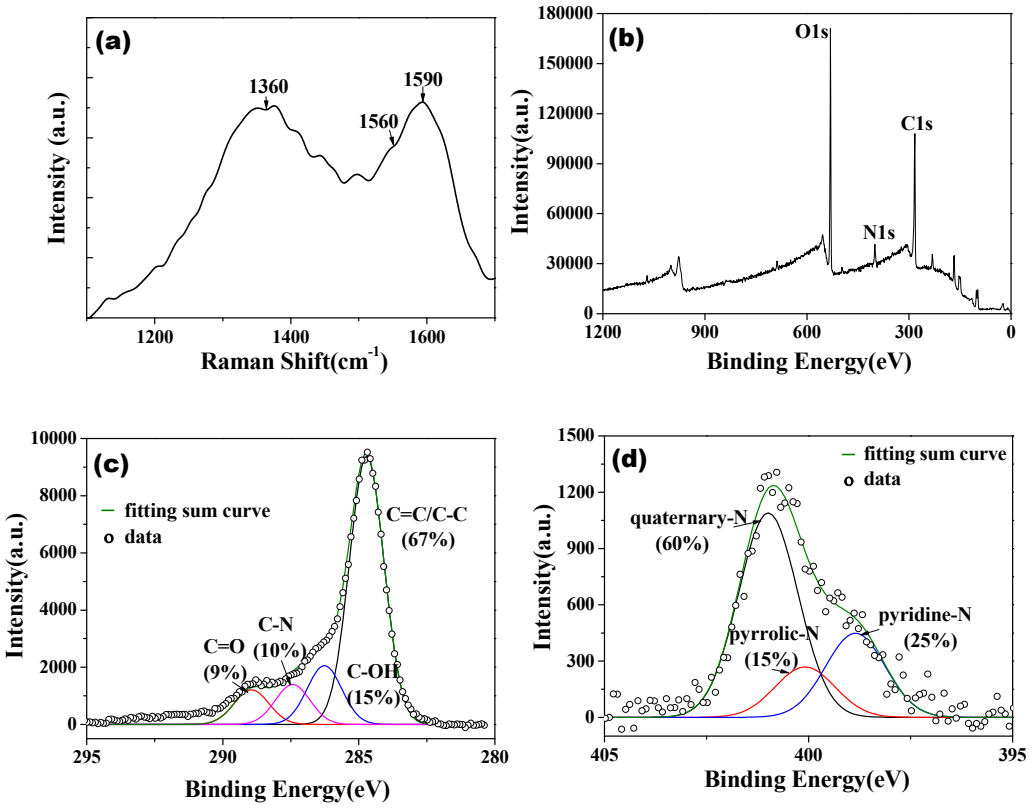

Figure 5. (a) Raman spectrum, (b) XPS survey spectrum, (c) XPS C1s spectrum, and (d) XPS N1s spectrum of the carbonaceous film. The fraction of the carbon- and nitrogen-containing species is provided in the parentheses.

Extensive graphitization of the copolymer occurred upon pyrolysis, as evidenced by Raman scattering spectroscopy (Figure 5a). The spectrum includes typical partially graphitic carbon fingerprints and suggests the presence of disordered carbon species [7,8], including a relatively narrow band around 1590 cm^{-1} corresponding to graphitic sp^2-hydribized carbon species (G-band), and a broader band around 1360 cm^{-1} corresponding to sp^3-hydribized carbon species (D-band). The G-band peak at 1590 cm^{-1} can be ascribed to crystalline graphite, for which the phenyl groups of the PS core could serve as precursors. The smaller band around

1560 cm^{-1} was previously assigned to imperfect crystalline graphite, which suggests that the nitrogen atom from the pyridyl groups of the arborescent copolymers acted as a defect site during carbonization [7]. The elemental composition of the carbonized films was measured by XPS. In Figure 5a, the survey spectrum reveals the presence of C (53.5 at%, atomic percentage), O (41.5 at%) and N (5 at%). The substantial amount of O detected likely originated from partial oxidation during the UV crosslinking step, since UV irradiation was carried out in air. The ratio of carbon to nitrogen atoms was ~10:1, indicating a rich nitrogen content for the carbonized arborescent copolymer films. The C_{1s} spectrum (Figure 5b) indicates the presence of three different types of carbon bonds: graphitic (283.4 eV), nitrous (286.1 eV), and oxygenated (287.7 eV). The asymmetric N_{1s} spectrum has three peaks at 398.9, 400.1 and 400.9 eV, which are attributed to pyridinic-N, pyrrolic-N, and graphitic-N, respectively. The presence of pyridinic-N was expected, but it appears that the pyridine rings were also transformed into other types of nitrogen-containing groups such as pyrrolic (400.3 eV) and quaternary (401.3 eV) nitrogen species, as suggested in a previous report for carbonized PS–*block*–P2VP micelles [8].

Conclusions

Atomic force and scanning electron microscopy were employed to visualize the molecular organization of arborescent PS–*graft*–P2VP copolymers in monolayer films spin casted onto silicon wafers. The uniformity of the copolymer films was influenced by the solvent selected. While the copolymers are known to be well-dispersed in methanol at low concentrations, methanol solutions of the copolymers led to non-uniform films with large aggregates and voids. Tetrahydrofuran, a good solvent for both the PS and P2VP components, resulted in uniform copolymer molecule arrays in the films. The macromolecules were strongly

flattened by adsorption forces, but recovered their spherical geometry upon water annealing. The water-annealed films of arborescent copolymers were useful as precursors for the preparation of carbon nanodots on an underlying continuous carbon film. Water annealing of the film prior to pyrolysis was found essential to maintain a "dots-on-film" surface topology. The pyrolyzed nanomaterials exhibited characteristics of partially graphitic carbon with nitrogen.

Acknowledgements

M. Gauthier gratefully acknowledges funding from the Natural Sciences and Engineering Research Council of Canada (NSERC) for the work.

References

[1] S.J. Teertsra, M. Gauthier, Dendrigraft polymers: macromolecular engineering on a mesoscopic scale, Prog. Polym. Sci. 29 (2004) 277–327, doi:10.1016/j.progpolymsci.2004.01.001.

[2] S.I. Yun, K.C. Lai, R.M. Briber, S.J. Teertsra, M. Gauthier, B.J. Bauer, Conformation of arborescent polymers in solution by small-angle neutron scattering: segment density and core-shell morphology, Macromolecules 41 (2008) 175−183, doi:10.1021/ma7021106.

[3] S.S. Sheiko, M. Gauthier, M. Möller, Monomolecular films of arborescent graft polystyrenes, Macromolecules 30 (1997) 2343−2349, doi:10.1021/ma9616064.

[4] M. Gauthier, J. Li, J. Dockendorff, Arborescent Polystyrene-graft-poly(2-vinylpyridine) copolymers as unimolecular micelles. Synthesis from acetylated substrates, Macromolecules 36 (2003), 2642–2648, doi:10.1021/ma021109p.

[5] S.I. Yun, R.M. Briber, R.A. Kee, M. Gauthier, Small-angle neutron scattering of arborescent polystyrene-graft-poly(2-vinylpyridine) copolymers, Polymer 44 (2003) 6579–6587, doi:10.1016/S0032-3861(03)00655-4.

[6] Beom Jin Kim and Ji Young Chang, Preparation of Carbon Nanospheres from Diblock Copolymer Micelles with Cores Containing Curable Acetylenic Groups, Macromolecules 39 (2006) 90–94, doi:10.1021/ma051713a.

[7] J. Huang, C. Tang, H. Lee, T. Kowalewski, K. Matyjaszewski, A novel route for the preparation of discrete nanostructured carbons from block copolymers with polystyrene segments, Macromol. Chem. Phys. 208, (2007) 2312–2320, doi:10.1002/macp.200700355.

[8] D.A. Rider, K. Liu, J.-C. Eloi, L. Vanderark, L. Yang, J.-Y. Wang, D. Grozea, Z.-H. Lu, T. P. Russell, I. Manners, Nanostructured magnetic thin films from organometallic block copolymers: pyrolysis of self-assembled polystyrene-blockpoly(ferrocenylethylmethylsilane), ACS Nano 2 (2008) 263□270, doi:10.1021/nn7002629.

[9] C. Tang, K. Qi, K.L. Wooley, K. Matyjaszewski, T. Kowalewski, Well-defined carbon nanoparticles prepared from water-soluble shell cross-linked micelles that contain polyacrylonitrile cores, Angew. Chem. Int. Ed. 43 (2004) 2783–2787, doi:10.1002/anie.200353401.

[10] T. Kowalewski, N.V. Tsarevsky, K. Matyjaszewski, Nanostructured carbon arrays from block copolymers of polyacrylonitrile, J. Am. Chem. Soc. 124 (2002) 10632−10633, doi:10.1021/ja0178970.

[11] C. Tang, A. Tracz, M. Kruk, R. Zhang, D.-M. Smilgies, K. Matyjaszewski, T. Kowalewski, Long-range ordered thin films of block copolymers prepared by zone-casting and their thermal conversion into ordered nanostructured carbon, J. Am. Chem. Soc. 127 (2005) 6918–6919, doi:10.1021/ja0508929

[12] Y. Wang, J. Liu, S. Christiansen, D.H. Kim, U. Gösele, M. Steinhart, Nanopatterned carbon films with engineered morphology by direct carbonization of UV-stabilized block copolymer films. Nano Lett. 8 (2008) 3993–3997, doi:10.1021/nl802554h.

[13] Y.H. Jang, S. T. Kochuveedu, Y. J. Jang, H.-Y. Shin, S. Yoon, M. Steinhart, D. H. Kim, The fabrication of graphitic thin films with highly dispersed noble metal nanoparticles by direct carbonization of block copolymer inverse micelle templates, Carbon 49 (2011) 2120–2126, doi:10.1016/j.carbon.2011.01.049.

[14] Y.-H. Lu, J.-Y. Liou, C.-F. Lin, Y.-S. Sun, Electrocatalytic activity of a nitrogen-enriched mesoporous carbon framework and its hybrids with metal nanoparticles fabricated through the pyrolysis of block copolymers, RSC Adv. 5 (2015) 105760–105773, doi:10.1039/c5ra22528k.

[15] Y.-S. Sun, W.-H. Huang, J.-Y. Liou, Y.-H. Lu, K.-C. Shih, C.-F. Lina, S.-L. Cheng, Conversion from self-assembled block copolymer nanodomains to carbon nanostructures with well-defined morphology, RSC Adv. 5 (2015) 105774–105784, doi:10.1039/C5RA17500C.

[16] Y.-S. Sun, W.-H. Huang, C.-F. Lin, S.-L. Cheng, Tailoring carbon nanostructure with diverse and tunable morphology by the pyrolysis of self-assembled lamellar nanodomains of a block copolymer, Langmuir 33, (2017) 2003−2010, doi:10.1021/acs.langmuir.6b04410.

[17] M. Kopeć, R. Yuan, E. Gottlieb, C.M.R. Abreu, Y. Song, Z. Wang, J.F.J. Coelho, K. Matyjaszewski, T. Kowalewski, Polyacrylonitrile-b-poly(butyl acrylate) block copolymers as precursors to mesoporous nitrogen-doped carbons: synthesis and nanostructure, Macromolecules 50 (2017) 2759−2767, doi:10.1021/acs.macromol.6b02678.

[18] C. Tang, B. Dufour, T. Kowalewski, K. Matyjaszewski, Synthesis and morphology of molecular brushes with polyacrylonitrile block copolymer side chains and their conversion into nanostructured carbons, Macromolecules 40 (2007) 6199–6205, doi:10.1021/ma070892o

[19] R. Yuan, M. Kopeć, G. Xie, E. Gottlieb, J.W. Mohin, Z. Wang, M. Lamson, T. Kowalewski, K. Matyjaszewski, Polymer accepted, doi:10.1016/j.polymer.2017.03.040.

[20] G. Liu, X. Li, J.-W. Lee, B.N. Popov, A review of the development of nitrogen-modified carbon-based catalysts for oxygen reduction at USC, Catal. Sci. Technol. 1 (2011) 207–217, doi:10.1039/C0CY00053A.

[21] Haibo Wang, Thandavarayan Maiyalagan, and Xin Wang, Review on recent progress in nitrogen-doped graphene: synthesis, characterization, and its potential applications, ACS Catal. 2 (2012) 781−794, doi:10.1021/cs200652y.

[22] L. Dai, Y. Xue, L. Qu, H.-J. Choi, J.-B. Baek, Metal-Free Catalysts for Oxygen Reduction Reaction, Chem. Rev. 2015, 115, 4823−4892, doi:10.1021/cr5003563.

[23] C. Sinturel, M. Vayer, M. Morris, M.A. Hillmyer, Solvent vapor annealing of block polymer thin films, Macromolecules 46 (2013) 5399–5415, doi:10.1021/ma400735a.